10.1098/rsta.2000.0688

THE ROYAL SOCIETY

# Crystalline structure and physical properties of ship superstructure spray ice

By Charles C. Ryerson and Anthony J. Gow

*Department of the Army, Cold Regions Research and Engineering Laboratory (CRREL), Corps of Engineers, Hanover, NH 03755-1290, USA*

In February and March 1990 the US Army Corps of Engineers Cold Regions Research and Engineering Laboratory (CRREL) made measurements of superstructure ice on a US Coast Guard cutter in the Bering Sea. Twenty-three ice samples were removed from bulkheads, decks and icicles during two icing events. Ice crystal measurements included crystal size, shape, orientation, brine-pocket location, size and shape, internal layering, and air-bubble sizes. Ice property measurements included salinity, density and temperature, with computed estimates of air and brine volume. This paper describes crystal and physical properties of the accreted ice and their relationship to ice sample position on the ship.

Texturally, accreted ice resembled frazil ice that forms from the consolidation of freely nucleated ice crystals in sea water. This resemblance is also reflected in bulk salinities, ranging from 24‰ to 7‰, compared with frazil formed during the initial stages of freezing of sea water, where bulk salinities can exceed 10‰. Crystalline structures of accreted ice ranged from rounded to polygonal. Generally, rounded crystals would be expected for ice formed from sea-spray droplets, polygonal crystals may be attributed to thermally driven modification. No trend towards reorientation of crystallographic *c*-axes in either freshly accreted or thermally modified ice was observed. Mean crystal sizes ranged from 0.56 mm to 1.15 mm, with even larger crystals in icicles.

Ice salinity averaged *ca.* 12‰ on bulkheads and *ca.* 21‰ on decks. Ice densities ranged from 0.69 to 0.92 Mg $m^{-3}$ and were generally higher on decks. Bulkhead ice had larger computed total porosity and air volume and lower brine volume than deck ice. Samples taken from decks and bulkheads generally compared well with Russian and Japanese measurements.

**Keywords: saline spray ice; ship icing; ice crystals; porosity; salinity; density**

## 1. Introduction

Ship superstructure ice results when water is deposited by bow spray in subfreezing temperatures. Patterns of ice accretion on a ship, and the properties of that ice, are a result of the integrated effects of spray frequency, spray liquid-water content, drop size, wind speed and direction, superstructure shape, ship speed, and other ship, weather and sea conditions. The result of ice formation is a deposit that increases weight and raises centre of mass, hinders deck activities, reduces seaworthiness by its effects on ship centre of gravity and freeboard, and decreases the overall efficiency of ship operations.

Few specifics are known about the physical properties of spray ice after it is deposited on ships, especially its crystalline structure. Detailed measurements of physical properties of spray-deposited ice were made by the Soviets on medium-sized fishing trawlers in the 1960s (Panov 1972; Golubev 1972; Smirnov 1972; Kultashev *et al*. 1972). Numerous Japanese measurements have been made on ships ranging in size from trawlers to patrol boats (Ono 1968; Tabata *et al*. 1963; Iwata 1973). Supplementary work has been done in saline wind tunnels, especially to measure salinity, brine volume and porosity (Makkonen 1987; Gates *et al*. 1986), and with models to simulate ice-accretion amount with location on the superstructure, and icicles (Lozowski *et al*., this issue). To our knowledge, measurements have not been made on ships in the Western Hemisphere, and none have been made on large ships except by Ryerson (1995). Ice properties and crystal structure affect the mass and thickness of ice accreted on decks and bulkheads, and the strength of ice requiring removal. They also provide information about the history of the ice and its depositional environment.

Properties of saline ice formed by direct freezing of ocean water, and its evolution with time and location, are reasonably well understood (Weeks & Ackley 1982; Mellor 1983) compared with spray-accreted saline ice. Saline spray ice freezes rapidly compared with floating sea ice, forms on vertical surfaces in addition to horizontal surfaces, grows in an environment where crystal growth is inhibited by a solid rather than liquid substrate, and is periodically flushed and dried as spray lofts over the bow and brine drains from ice at higher locations on the superstructure. This unique energy and mass environment for saline ice growth and evolution impacts on the mass of ice at various locations on the ship, especially at higher levels where ship dynamics are most affected. It also impacts on ice strength, physical and crystalline properties.

Ryerson (1995) addressed properties of spray, and the dynamics of ice growth and ablation on a large US Coast Guard cutter (USCGC). This paper characterizes the crystalline and physical properties of spray ice accreted on the same ship, and changes with location and the accretion environment.

## 2. Background

Ice samples were collected during a research cruise in the Bering Sea during February and March 1990 aboard the 2703 t displacement, 115 m long USCGC *Midgett* (Ryerson & Longo 1992; Ryerson 1995). Twenty-three ice samples were removed from decks, bulkheads, 5″ gun and lines during two icing events. One icing event occurred from 22 to 25 February, and the second from 10 to 14 March. Ice samples were removed from the *Midgett*'s decks and bulkheads on 24 February and 12 and 13 March (three times during the latter event) (figure 1, table 1). As indicated in figure 1, all samples were taken on and around the forecastle because insufficient ice for sampling accreted elsewhere.

Samples were removed in complete sections, using a putty knife, from the substrate surface, which was either painted steel, painted aluminium, non-skid or polypropylene-covered cables. Samples were immediately placed in clear plastic freezer bags and sealed to prevent contamination, and to prevent draining brine from escaping. Though many samples appeared to be nearly saturated with water, such as samples removed from the forecastle deck surface, no water ran freely from samples

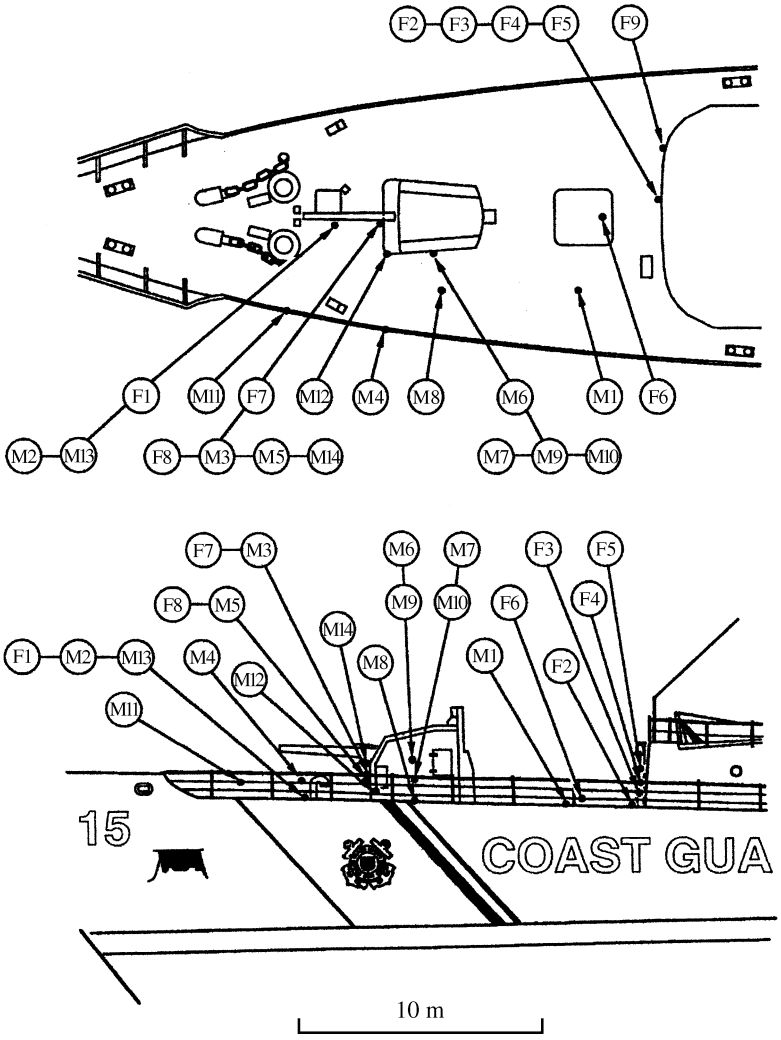


Figure 1. Ice sample locations on the USCGC *Midgett*. Letters refer to the sample month (F denotes February and M denotes March), and numbers denote sample number within the month (see table 1). Scale refers to drawings only.

Table 1. *Ice sample properties*

| sample[a] | accretion surface | accretion orientation | thickness (cm)[b] | bulk salinity (‰)[b] | density (Mg m$^{-3}$)[c] | air volume (%)[d] | brine volume (%)[d] | porosity (%)[d] |
|---|---|---|---|---|---|---|---|---|
| F1 | deck | horizontal | 3.2 | 24.0 | 0.895 @ −9.3 °C | 5.5 | 13.7 | 19.2 |
| F2 | deck | horizontal | 2.8 | 21.1 | 0.888 @ −6.6 °C | 6.2 | 15.8 | 22.0 |
| F3 | bulkhead | vertical | 1.6 | 14.7 | 0.768 @ −7.5 °C | 18.0 | 8.5 | 26.5 |
| F4 | bulkhead | vertical | 1.6 | 14.1 | 0.762 @ −7.8 °C | 18.6 | 7.9 | 26.5 |
| F5 | bulkhead | vertical | 2.0 | 13.0 | 0.823 @ −8.5 °C | 11.9 | 7.3 | 19.2 |
| F6 | DTMB[f] hatch | horizontal | 1.8 | 24.2 | 0.917 @ −8.0 °C[e] | 3.3 | 15.9 | 19.2 |
| F7 | 5″ gun | vertical | 2.8 | 16.2 | 0.773 @ −8.0 °C[e] | 17.6 | 9.0 | 26.6 |
| F8 | 5″ gun | vertical | 3.0 | 13.7 | 0.718 @ −8.0 °C[e] | 23.2 | 7.1 | 30.3 |
| F9 | DTMB[f] bulkhead | vertical | 1.9 | 11.5 | 0.693 @ −8.0 °C[e] | 25.7 | 5.7 | 31.4 |
| M1 | deck | horizontal | 0.6 | 24.9 | — | — | — | — |
| M2 | deck | horizontal | 0.6 | 25.4 | — | — | — | — |
| M3 | 5″ gun | vertical | 1.1 | 14.8 | 0.848 @ −2.2 °C | 11.3 | 30.1 | 41.4 |
| M4 | life line | hanging | — | 16.7 | — | — | — | — |
| M5 | 5″ gun | vertical | 0.6 | 10.3 | 0.871 @ −1.6 °C | —[g] | —[g] | —[g] |
| M6 | 5″ gun | vertical | 0.8 | 7.9 | 0.799 @ −1.6 °C | —[g] | —[g] | —[g] |
| M7 | 5″ gun | vertical | 1.2 | 8.6 | 0.872 @ −1.6 °C | —[g] | —[g] | —[g] |
| M8 | deck | horizontal | 4.4 | 16.2 | 0.868 @ −2.4 °C | 9.3 | 30.8 | 40.1 |
| M9 | 5″ gun | vertical | 2.3 | 7.5 | 0.877 @ −3.0 °C | 6.0 | 11.5 | 17.5 |
| M10 | 5″ gun | vertical | 3.4 | 7.0 | 0.882 @ −3.0 °C | 5.3 | 10.8 | 16.1 |
| M11 | life line | hanging | — | 11.8 | — | — | — | — |
| M12 | 5″ gun icicles | hanging | — | 14.2 | — | — | — | — |
| M13 | deck | horizontal | 2.4 | 13.7 | 0.865 @ −1.6 °C | 10.3 | 40.1 | 50.4 |
| M14 | 5″ gun | vertical | 1.1 | 9.8 | 0.827 @ −2.8 °C | 12.0 | 15.2 | 27.2 |

[a]Sample identifier (figure 1). [b]Thickness and salinity measured at CRREL. [c]Temperature of ice measured *in situ* during sampling on USCGC *Midgett* (see figure 2 for air temperatures during sampling). Density measured at CRREL. [d]Computed volume of entrapped air and brine and total porosity at shipboard ice temperature (after Cox & Weeks (1983)). [e]Sample temperatures were estimated from the mean of other ice temperatures in same sample period. [f]'DTMB' refers to experimental ice removal panels installed by the US Navy David Taylor Model Basin (DTMB) atop main hatch cover and on portion of starboard forward bulkhead. [g]Temperature not known with sufficient accuracy for computations.

as they were lifted from the substrate, though the substrate itself was occasionally wet. Samples removed from bulkheads were always dry at the ice–substrate interface.

Samples were kept on deck in freezer bags during the duration of each sampling excursion, 30–60 min. They were then moved to the freezer compartment of the Officer's ward-room galley refrigerator, approximately amidships, by carrying the bagged ice through ship passages within an insulated container. The temperature of the freezer compartment was *ca.* −18 °C. From within minutes to a few hours samples were moved, again with the sample bags within an insulated container, from the ward-room galley freezer to the ship's main food locker, also at −18 °C (Ryerson & Longo 1992). Samples remained in the food locker within picnic coolers for the remainder of the cruise, until May 1990.

Immediately upon the ship's return to Alameda, CA, at the end of the cruise, the coolers of bagged ice were packed with dry ice. The bagged ice was kept sealed and separated from the dry ice by layers of cardboard. The coolers were then air-shipped to CRREL within 24 h and placed in cold storage. The ice was stored in cold rooms at temperatures of −12 to −30 °C for 6–7 months before initial analysis including density and salinity measurements and initial observations of the crystal structure in thin sections. Samples were prepared and analysed in cold rooms at temperatures ranging from −10 to −18 °C. In 1998, thin sections of the crystal structure were re-examined mainly to determine the sizes of crystals and inclusions and their relationships to one another.

Measurement of saline ice properties and structure are best made immediately after sampling, because brine drains rapidly from newly formed ice, and temperature changes or communication with the atmosphere can cause changes during transport and storage (Weeks & Ackley 1982). However, careful packing and storage can minimize problems and preserve the ice sufficiently for useful analyses at a later time.

## 3. Ice-accretion environment

Conditions that may affect the physical properties of accreted ice, either through rate of freezing during accretion, or after accretion, include air temperature, seawater temperature, seawater salinity, and wind speed. Information was obtained either directly or computed from the ship's logs.

Air temperatures sufficiently cold to freeze sea spray persisted for *ca.* 100 h during each of the two icing events (figure 2). The February icing event was colder than the March event, averaging −10.2 and −5.6 °C, respectively. Minimum and maximum temperatures were both higher in the March event, and temperatures lingered near freezing for at least 50% of the event. By contrast, temperatures in the February event remained below −10 °C for several days. In both events, wet-bulb temperatures always remained within a few degrees of the dry-bulb temperature, indicating generally high relative humidities.

In 117 cases of trawler icing along the east coast of North America, Ryerson (1991) found air temperatures averaging −8.1 °C, with 67% of all cases occurring between temperatures of −3.5 and −12.6 °C. Soviet studies indicate that icing rarely occurs at air temperatures above −3.0 °C, and most cases occur between temperatures of −4.1 and −10.1 °C. Japanese research has found icing to be most severe in air temperatures between −6.0 and −8.1 °C (Ono 1968). Both of the USCGC *Midgett* icing

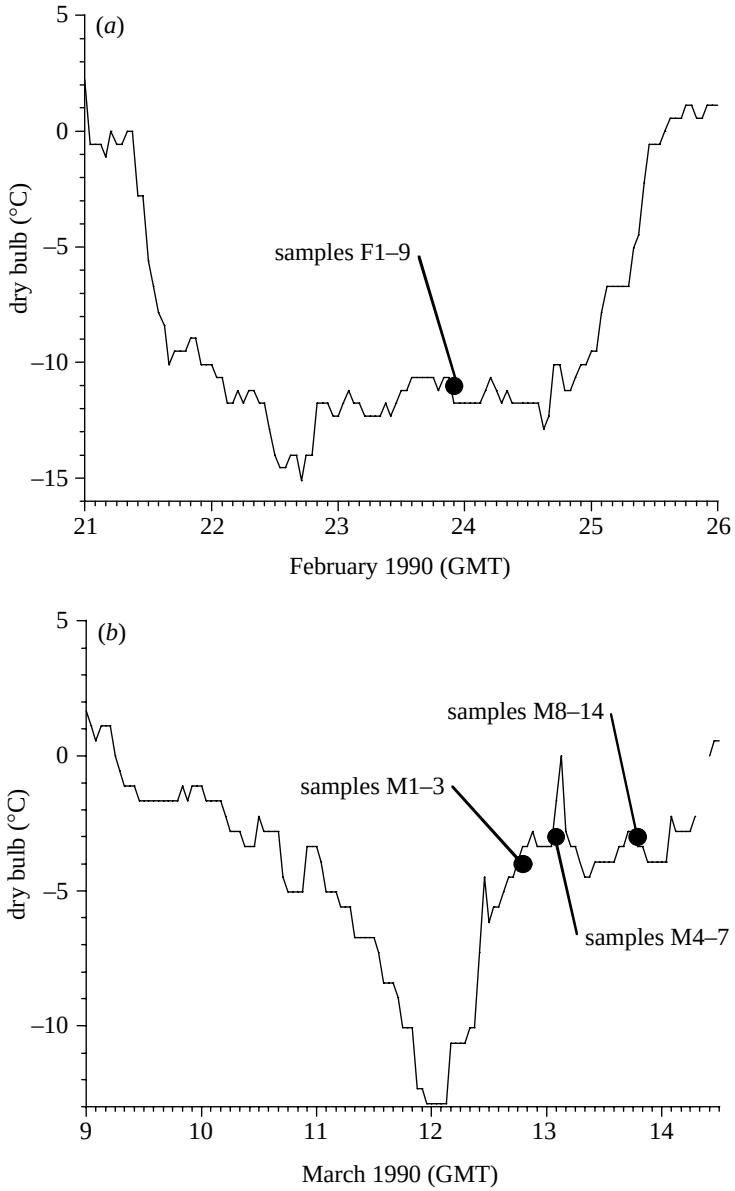


Figure 2. Air temperature and sampling times during February and March 1990 ice-accretion events in the Bering Sea. Sample numbers refer to figure 1 and tables 1 and 2. During each sampling period, all samples were collected within *ca.* 30–60 min of one another.

events fell well within temperature ranges observed by others during superstructure icing events.

Best estimates of seawater temperature were derived from measurements at the engine coolant intakes, by bathythermographs, and by bucket samples (Ryerson & Longo 1992; Ryerson 1995). Water temperatures averaged *ca.* 2.2 °C during the February event, and 0.6 °C during the March event. In a literature review, Shellard

Table 2. *Crystal and bubble size measurements*

(NM denotes not measured; LCs and SCs denotes large and small crystals, respectively.)

| sample | accretion surface | thin-section orientation | mean crystal area ($mm^2$) | RMS diameter (mm) | mean bubble diameter (mm) |
|---|---|---|---|---|---|
| F1 | deck | horizontal | 0.63 | 0.79 | 0.26 |
| F2 | deck | horizontal | 0.45 | 0.67 | 0.28 |
| F3 | superstructure vertical surface | vertical | 0.60 | 0.78 | 0.20 |
| F4 | superstructure vertical surface | vertical | 0.38 | 0.62 | NM |
| F5 | superstructure vertical surface | vertical | 0.40 | 0.63 | 0.23 |
| F6 | deck hatch | horizontal | 0.59 | 0.77 | 0.25 |
| F7 | 5″ gun forward face | vertical | 0.62 | 0.79 | 0.26 |
| F8 | 5″ gun forward face | vertical | 0.46 | 0.68 | 0.25 |
| F9 | superstructure vertical surface | vertical | 0.66 | 0.81 | 0.29 |
| M3 | superstructure vertical surface | vertical | 0.58 | 0.76 | 0.27 |
| M5 | 5″ gun forward face | vertical | 0.31 | 0.56 | 0.27 |
| M6 | 5″ gun forward face | vertical | 0.53 | 0.72 | NM |
| M8 | deck near 5″ gun | horizontal | 1.33 | 1.15 | 0.29 |
| M9 | 5″ gun vertical face, port side | vertical | 0.50 | 0.71 | 0.31 |
| M10 | 5″ gun vertical face, port side | vertical | 0.58 | 0.76 | 0.24 |
| M12 | icicles, 5″ gun mount | horizontal | 0.73 | 0.85 | 0.27 |
| M12 | icicles, 5″ gun mount | vertical | 2.66 (LCs)<br>0.83 (SCs) | 1.63 (LCs)<br>0.91 (SCs) | NM |
| M13 | deck near 5″ gun | horizontal | 3.53 (LCs)<br>1.06 (SCs) | 1.88 (LCs)<br>1.03 (SCs) | 0.25 |
| M14 | 5″ gun forward face | vertical | 1.05 | 1.02 | 0.24 |

(1974) found little agreement about the importance of seawater temperature and icing rates. Lower water temperatures contribute to heavier icing, but air temperature is an overriding factor. Ryerson (1991) found icing to be most common when seawater temperatures averaged 1.0 °C, with 67% of all cases occurring at temperatures between 3.0 and −1.0 °C. Jorgensen (1982) indicates that when wind speeds are high, and air temperatures are lower than −5.0 °C, seawater temperature has a negligible effect on icing rate.

Average seawater salinities were *ca.* 33‰ during the two icing events (Ryerson 1995). Though Shellard's (1974) review found the importance of seawater salinity to be small in affecting icing rate, others have found it to be important in assessing the mass and thermodynamics of icing (Brown & Roebber 1985). Jorgensen (1982) reports icing to begin at higher temperatures when salinities are lower. Makkonen (1987) and Gates *et al.* (1986) make a strong case about the affect of salinity on the 'sponginess' of ice, its thermodynamics and mass. The seawater salinities and their variation observed aboard the *Midgett* fall well within values observed in other ship icing studies (Shellard 1974).

Relative wind speeds across the bow were computed from true wind speed, ship speed and true wind direction (Ryerson & Longo 1992). Relative wind velocities were somewhat larger in the February event, with a maximum of 24.2 m $s^{-1}$. Relative winds, as measured on the Beaufort scale, averaged from force 5 to force 6 for the two events, with a maximum of force 9 during the February icing event, and force 8 during the March event. According to Jorgensen (1982), Beaufort forces 5–6 are the most common lower limits for ship icing. Ono (1968) found that relative winds produced the greatest icing, in concert with low temperatures, when velocities were greater than 10.8 m $s^{-1}$. Iwata (1973) observed icing on patrol boats at relative wind speeds of 10.3–20.6 m $s^{-1}$. Gashin observed the most intense icing on the trawler *Aysberg* when wind speeds were greater than 20.6 m $s^{-1}$ (Borisenkov & Panov 1972).

Spray drop sizes, which affect ice appearance and density (Jorgensen 1982) and perhaps initial ice crystal size, were measured with a stroboscopic camera system on the USCGC *Midgett*. About 7000 drops were measured through 39 representative spray events, to yield drops ranging from 14 to 7700 μm in diameter (Ryerson 1995). Mean median volume diameter for all 39 spray events was 1094 μm, ranging from 169 to 6097 μm for individual spray events.

## 4. Ice distribution

Superstructure ice never accreted to more than minimal thickness aboard the USCGC *Midgett* (table 1).

Samples of ice were taken at the end of the February icing event, but no samples were taken during the event (figure 2). Thicknesses of samples ranged from 3.2 cm at location F1 on the deck forward of the 5″ gun, to 1.6 cm on the forward bulkhead (table 1). During the March icing event samples were taken at three different times during the event (figure 2). Up to 4.4 cm of ice formed on the main deck during the March event, and 3.4 cm of ice on the port vertical surfaces of the 5″ gun housing. As in the February event, ice thicknesses, overall, were small, and most ice formed on the port side because, in both events, seas approached principally from port.

Mean thickness of ice on horizontal surfaces at the end of the February icing event was 2.6 cm, and average vertical surface thicknesses were 2.2 cm. During the March icing event, horizontal surfaces averaged 2.0 cm of ice, and vertical surfaces averaged 1.5 cm, indicating that vertical surface ice was *ca.* 75% of the thickness of horizontal surface ice (Ryerson 1995).

Automated ice-thickness time-series measurements on the ship, though not highly accurate in absolute terms, did provide trends in ice thickness through icing events (Ryerson 1995). These trends suggest that accretion and ablation sub-events occur within the primary ice-accretion event. Perhaps caused by changes in air tempera-

ture and seawater thermal flux, these sub-event patterns suggest that superstructure icing is not a simple accretion process, but a series of accretion–ablation episodes. These accretion–ablation sub-events could have an influence on resulting ice physical properties and crystallography.

## 5. Ice properties

### (*a*) *Density*

Ice used for measuring density and salinity was sectioned from the larger samples removed from the ship. Samples used for density measurements were sanded to a thickness of 1.2–3.2 cm. A bandsaw was used to cut the samples into rectangular slabs with sufficient width and length to yield finished samples containing *ca.* 50–340 $cm^3$ of ice. Each sample was measured with digital calipers to 0.02 mm accuracy at three locations in each dimension, and volume computed from the mean of each dimension. Ice mass was measured to the nearest 0.01 g, and density was computed on the basis of the measured masses and volumes of the samples. It is estimated that densities are correct to within ±1% of their true values. All ice samples were allowed to reach cold room temperature before measurements were made.

Ice density, coupled with thickness, determines the mass of ice at various locations on the ship. It also has a large effect upon the ultimate strength of the ice, and how well it adheres to the substrate (Smirnov 1972). Ice density for the *Midgett*'s February and March icing events ranged from 0.69 to 0.92 $Mg\,m^{-3}$ (table 1). Ice densities on horizontal surfaces were 1.2 times larger than on vertical surfaces in the February icing event, but there was no significant difference in March.

Kultashev *et al*. (1972) found the density of ice on Soviet fishing trawlers to vary between 0.71 and 0.967 $Mg\,m^{-3}$. Tabata *et al*. (1963) found densities on four ships, totaling 121 samples, to vary between 0.62 and 0.94 $Mg\,m^{-3}$. There was no systematic change of density with location on the four Japanese ships.

### (*b*) *Salinity*

Salinities of melted samples were measured with a temperature-compensating Beckman Solubridge. All salinities were corrected to a reference temperature of 25 °C . Measurement precision is estimated at ±0.2‰.

Mean ice bulk salinity on horizontal surfaces was *ca.* 8–10‰ larger than on vertical surfaces in both icing events (table 1). Ice samples were taken on the ship whenever there was an opportunity, thus the amount of time that brine drainage from the ice had occurred since the last splashing by sea water is unknown. However, during several sampling excursions in March, spray was being lofted over the ice sampling team as ice was being removed. In most cases the ice was no more than a few hours old since the last ice accretion had occurred. Panov (1972) found generally higher ice salinities from similar seawater salinities on a Soviet trawler than we found on the *Midgett*. On both horizontal and vertical surfaces, 10–12 h into an icing event, Panov's (1972) salinities ranged from 10.3 to 37.5‰.

### (*c*) *Porosity*

A significant portion of spray-accreted saline ice is often composed of unfrozen liquid water trapped within the ice matrix (Gates *et al*. 1986; Makkonen 1987). Termed

'spongy' ice, wind-tunnel experiments have demonstrated that unfrozen water content can total up to 50% of the mass of the deposit (E. Lozowski, personal communication). If the unfrozen brine eventually drains, as occurs quickly during and immediately after accretion and more slowly later, the mass of the accretion will be considerably reduced below what thickness alone may suggest.

The volumes of air and brine, collectively termed total porosity, of ice samples removed from the *Midgett* were computed using equations developed by Cox & Weeks (1983) and Frankenstein & Garner (1967). The volumes computed are estimates because the equations were developed for floating sea ice, not spray ice, and the answers rely upon density, salinity and temperature measurements that, with all potential errors considered, could cause uncertainty in the porosity estimates. The derived brine volumes and air contents are calculated for the *in situ* temperature for the accreted ice at the time of sampling (table 1).

Total porosity and its constituent air and brine volumes varied considerably between ice on vertical and horizontal surfaces, and between the February and March icing events. In the February event, total porosities were somewhat larger on vertical surfaces (table 1). Ice on all surfaces was cold in the February event, and samples were taken hours after spraying had ceased. Total ice porosity in the March event was much larger on horizontal surfaces than on vertical surfaces (table 1). During sampling, most ice in the March event was very wet because of continual splashing and warm temperatures, which may have contributed to higher porosity on the decks.

A larger proportion of pores are filled with brine on horizontal surfaces than on vertical surfaces in both events (table 1). Brine drains more readily from ice pores on vertical surfaces, which then fill with air. A larger proportion of March ice pores are filled with brine than are February pores. This may be the result of the higher temperatures in the March event (figures 2 and 3).

## 6. Ice structure

Few studies have examined the crystalline structure of ice created from bow spray. Ono (1968) sectioned ice removed from handrails of the patrol boat *Chitose* and photographed crystals through polarizing filters. He found tiny crystals, *ca.* 0.5 mm in diameter, with random orientations. The only other study, conducted by Golubev (1972), was quite thorough, and examined the relationship between crystal structure and orientation of the icing surface, substrate material, distance within the ice from the substrate, and air temperature. Golubev's work was done on a medium-size Soviet fishing trawler in the Sea of Japan.

Several ice structure characteristics were examined from the *Midgett* samples, including ice crystal shape, size and orientation, and inclusion size and shape. The February icing event is the least difficult to analyse because temperatures were cold during the entire period. The warm temperatures late in the March event complicate understanding of ice characteristics during the second event (figure 2).

## 7. Microstructural studies of accreted ice

Samples for microstructural analysis were prepared by freezing samples of accreted ice onto glass slides and then reducing them to the requisite thickness on a microtome. Initially, these sections were thinned to 1–2 mm thickness and then photographed.

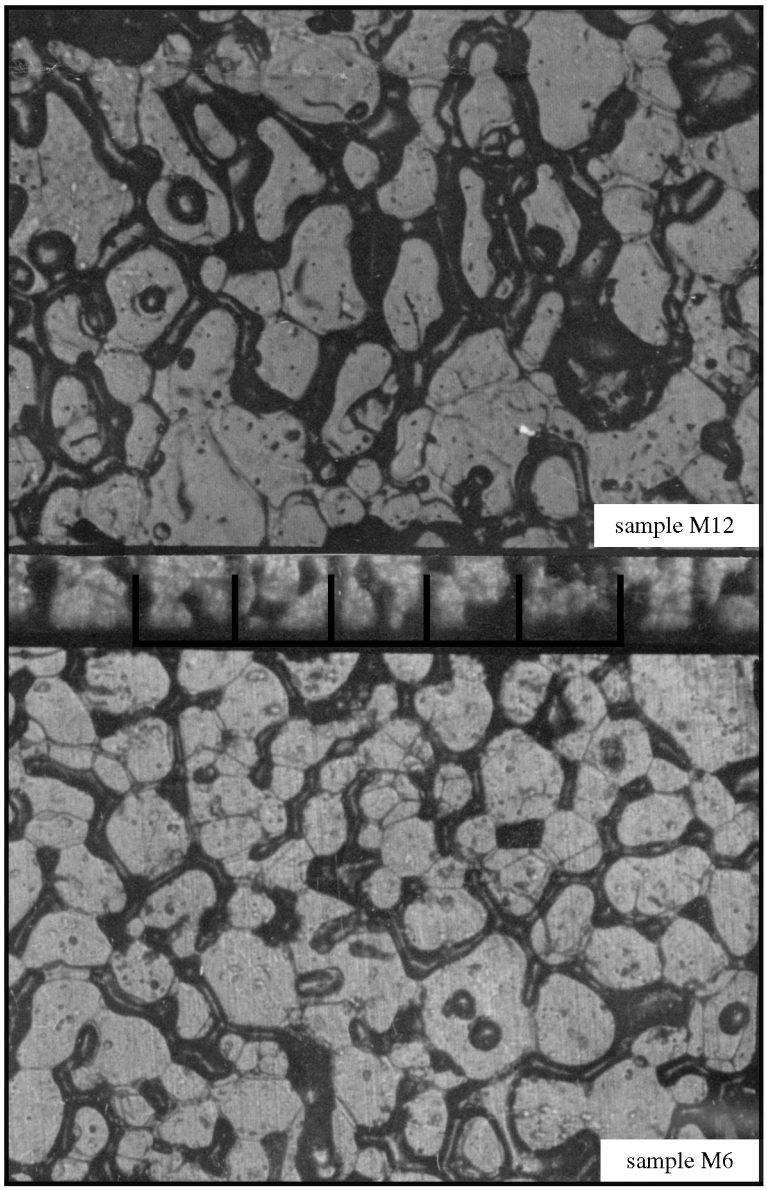


Figure 3. Thin sections of ice sampled during the March icing event from a bulkhead (M6) and an icicle (M12), illustrating grains encircled by large channelized networks filled with brine (scale in mm).

However, in order to improve the resolution of the microstructure for crystallographic examination, additional microtoming was performed until the sections measured 0.5 mm or less in thickness, depending on the average size of crystals in the section. Sections were prepared both parallel and normal to the accretion surface. A Baush and Lomb extension (bellows) camera fitted with polarizers was used to obtain structure photographs of each thin section. Photographs were taken at 7.5× magnifi-

cation on sheet film measuring 17.5 cm × 12.5 cm. Contact prints, which constitute a ready source of structure pictures that can be compared and evaluated at a moment's notice, were used to document textural characteristics of the accreted ice (crystal–inclusion relationships) and to measure crystal and inclusion sizes.

## 8. Crystal size measurements

The determination of crystal size in thin sections usually involves measurement of either the diameter or the cross-sectional area of grains. Seligman (1949), for example, used a method of least-circle diameters to measure grain sizes in rubbings of ice. Ahlmann & Droessler (1949) measured the shortest and longest axes of ice grains to obtain average cross-sectional areas. Schytt (1958) and Stephenson (1967) employed much the same technique to measure crystal sizes in Antarctic firn. These methods all suffer from the problem that a section seldom cuts crystals at their maximum (true) diameter, leading to underestimates of the true sizes of crystals. Variations in particle size also complicate the problem, which is further compounded by the lack of knowledge concerning the distribution of particle sizes within the original sample. Since under-sized cuts of crystals in a thin section exert a disproportionate influence on the average particle size, it was decided to restrict measurements of crystal size in accreted ice to the 50 largest crystals in a given area of the section, as advocated by Gow (1987).

As applied to the samples of accreted ice obtained on the cruise of the USCGC *Midgett*, an area of 10 cm × 8 cm on the enlarged print (17.5 cm × 12.5 cm) was used to select the 50 largest crystals. This selection of crystals generally constituted less than 25% of the total number of crystals in the 10 cm × 8 cm area of the contact print. Actual values of the cross-sectional areas of crystals were calculated from measurements of length and breadth made with a pocket comparator, which, allowing for the 7.5× magnification of the contact print, permitted measurements to the nearest 0.05 mm. The mean cross-sectional areas of crystals ($mm^2$) were then converted to root-mean-square (RMS) diameters (mm). This measurement method was preferred to the intercept method because of the substantial corrections needed to account for intersected inclusions, both air bubbles and brine channels, which occur abundantly in accreted ice. With the exception of one or two thin sections, crystal size measurements reported here were restricted to sections cut parallel to the accreting surface.

## 9. Inclusion size measurements

Measurements of air bubble dimensions were also attempted in the majority of thin sections, despite the intrinsic difficulty of distinguishing air bubbles from brine pockets trapped in the ice. Although this distinction between these two principal types of inclusion trapped in the ice is difficult to establish with certainty, inclusions we identified as air bubbles tended to occur either along grain boundaries or at multigrain intersections. We concentrated our measurements of bubble size on spherical inclusions, which we believe are more likely to represent air bubbles than brine pockets. Small rounded inclusions were frequently observed within crystals. This might be interpreted as evidence of incidental grain growth (recrystallization) that most likely occurred in the accreted ice some time after its formation but prior to sampling or sectioning.

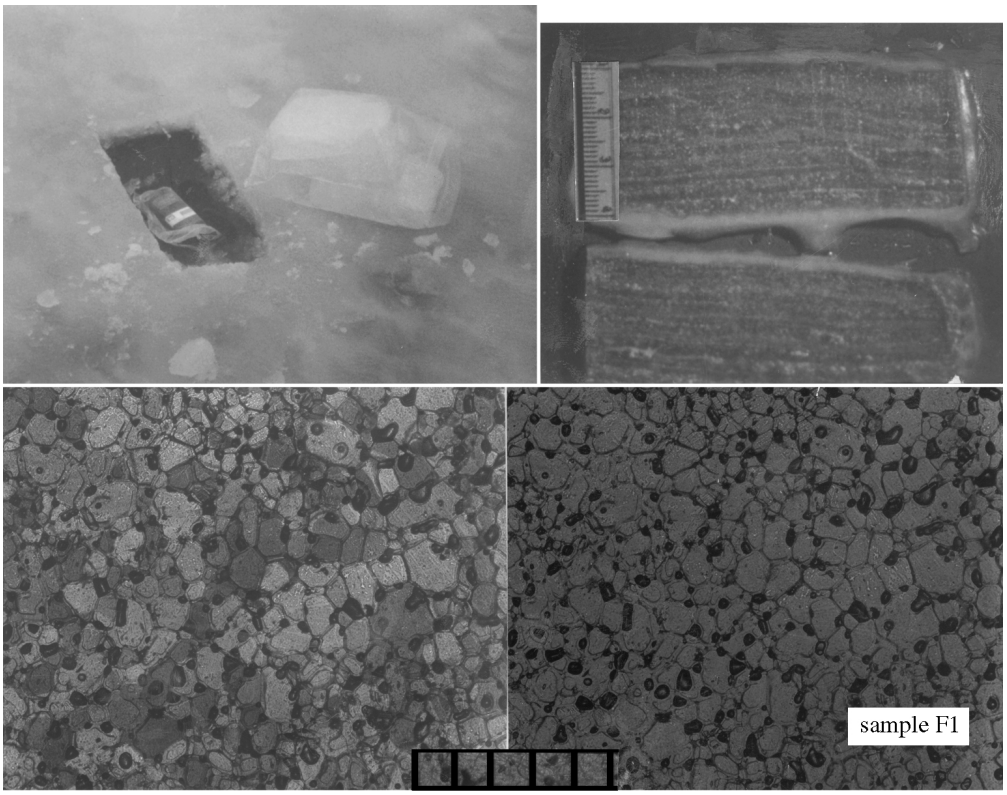


Figure 4. Sample F1 taken from the main deck during the February icing event. Photos clockwise from top left show the sample location, vertical thick sections in natural light, horizontal thin section in natural light, and horizontal thin section under crossed polarizers. Note layering in thick sections. Dark circular inclusions in thin sections are air bubbles (scale in mm).

## 10. Crystal orientation observations

No attempt was made to determine preferred crystal orientation using universal stage techniques. However, it appeared from examining the general nature of interference colour changes in the crystal aggregates when a section was rotated between crossed polarizers that *c*-axis orientations were substantially random. Dimensional orientation of crystals was, however, observed in sections cut from icicles. Results of crystal size measurements of 19 of the 23 samples collected during the cruise are presented in table 2; also, bubble sizes were obtained for 16 of the 19 samples sectioned for microstructural analysis.

Descriptions of the microstructural characteristics of a selection of samples of accreted ice follow.

## 11. Results of microstructural examination

### *Sample* F1

A deck sample, as indicated in figure 4, of 3.2 cm thick ice with a mean density of 0.895 Mg m$^{-3}$ and characterized by a high salinity of 24.0‰. The salinity data, in

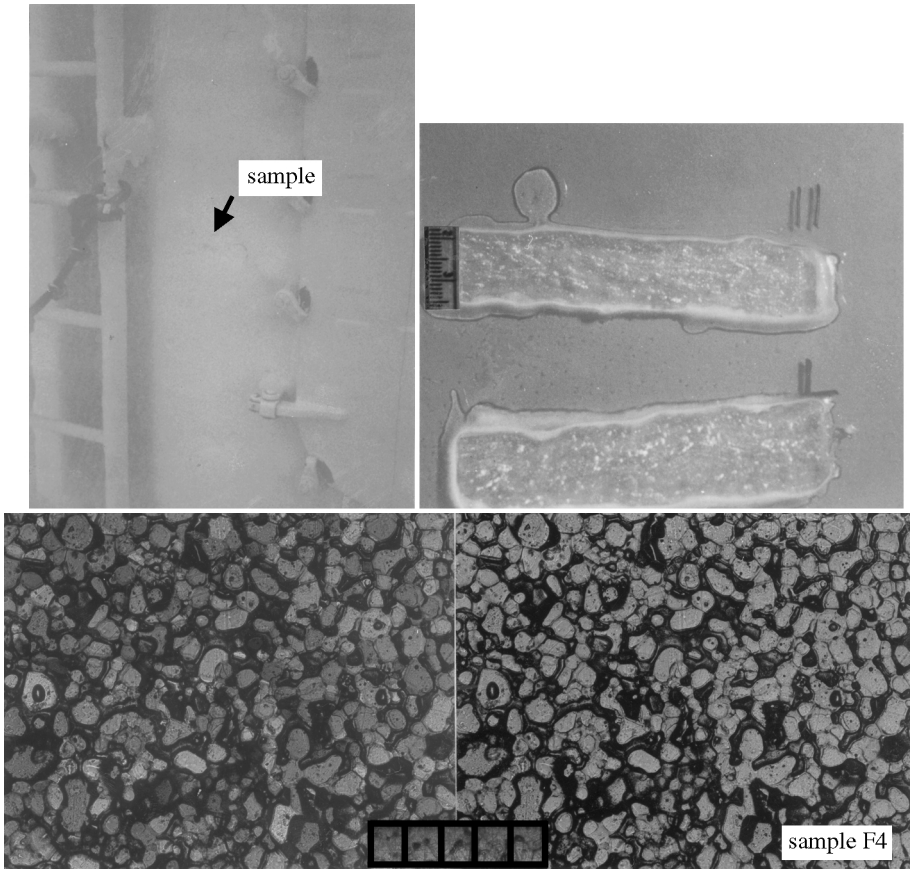


Figure 5. Sample F4 taken from the forward bulkhead on the main deck. Clockwise pictures show sample location between the left door edge and the ladder midway between the first and second dog above the door hinge (see arrow), vertical thick sections, horizontal thin sections photographed in natural light and between crossed polarizers. Note rounded shape of ice crystals (scale in mm).

conjunction with the *in situ* temperature of the accreted ice and its density, yielded a total porosity of 19.2%, consisting of 13.7% of brine by volume and an entrapped air content of 5.5%. Vertical thick-section slices in figure 4 clearly demonstrate the layered nature of the ice, which may be associated with the episodic spraying and drying process of sea-spray accretion, or with the sloshing of water across the deck, trapped by frozen scuppers as the ship rolls. The mean cross-sectional area of crystals measured 0.63 $mm^2$, equivalent to a RMS diameter of 0.79 mm. Crystals are generally subrounded, though some straightening of the grain boundaries is also apparent. A variety of inclusion structures are present, either concentrated along grain boundaries or located at multigrain intersections. Larger, often irregularly shaped inclusions are identified as brine pockets; smaller, generally rounded inclusions are tentatively identified as air bubbles. Bubbles average 0.26 mm in diameter or about one-third that of the crystals. Crystal orientation is random, based on observations of the interference colours when the thin section is rotated between crossed polarizers.

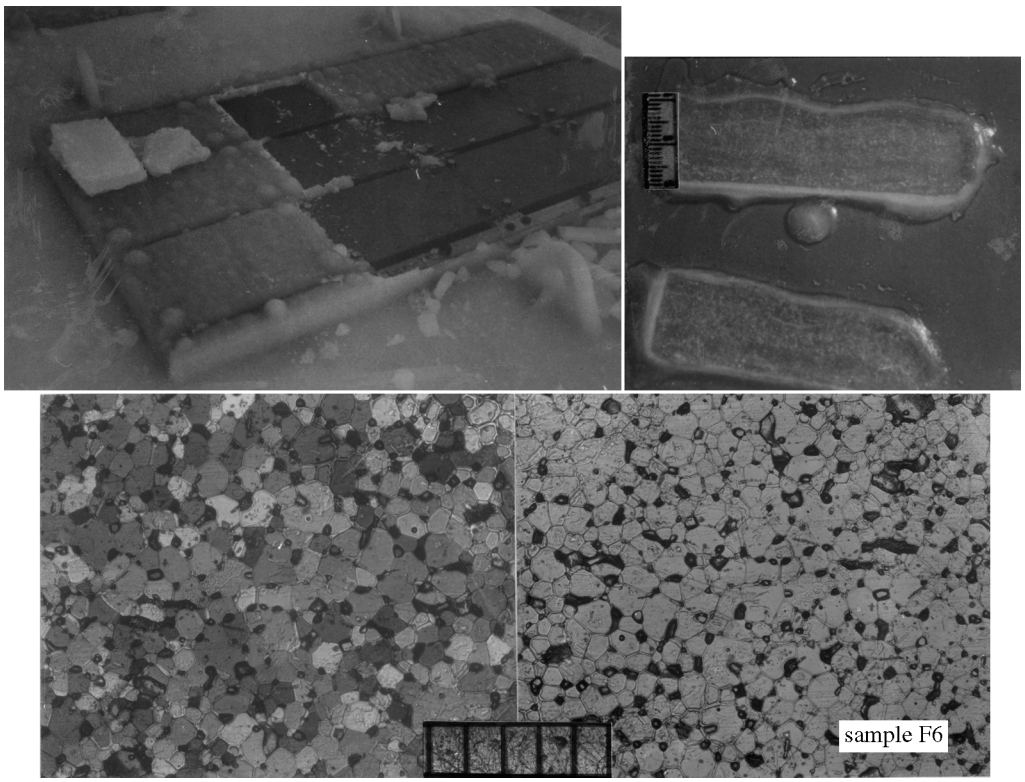


Figure 6. Sample F6 taken from the ice-accretion panel on the main deck hatch. Clockwise pictures show sample location, thick-section layering, and modified ice crystal boundaries photographed in natural light (right) and between crossed polarizers (left). Dark circles in thin sections are air bubbles (scale in mm).

### *Sample* F4

A bulkhead sample, 1.6 cm thick, was retrieved 1 m above the deck (figure 5). The vertical thick section shows little evidence of layering. Horizontal thin-section grains can be seen to posses generally rounded outlines. Multi-crystalline grains occur abundantly in sample F4, and the mean crystal cross-section, 0.38 $mm^2$, was the smallest measured in the February icing series. A salinity of 14.1‰ was measured. Derived values of brine and entrapped air volume calculated at the *in situ* temperature of −7.8 °C are 7.9% and 18.6%, respectively.

### *Sample* F6

This sample (figure 6), measuring 1.8 cm thick, was obtained from the top of the hatch on the US Navy DTMB ice-accretion panel on the main deck (table 1). DTMB had placed panels on the main deck hatch cover, and on the starboard side of the forward bulkhead, to experiment with ice-removal techniques. These panels stood several centimetres off of the hatch cover and bulkhead surfaces, which allowed cold air to circulate behind the panels, keeping them colder than the hatch cover or bulkhead. The thick-section photograph displays wavy layering. Though microstructurally similar to the deck-accreted ice at sampling site F1, many of the crystals are

seen to possess straight boundaries that frequently intersect at angles of *ca.* 120°. This near-equilibrium intersection angle for ice crystals is compatible with some process of recrystallization, possible at elevated temperatures while the ice was still accreted to the hatch. Such a process has been well documented by Gow (1987). Mean crystal cross-sectional area (0.59 $mm^2$) and derived mean diameter (0.77 mm) are very similar to values measured on sample F1. Bubble sizes (averaging 0.25 mm) are also very close to those found for sample F1. Numerous irregularly shaped inclusions are identified as brine pockets. Bulk salinity is essentially the same as that measured on sample F1 (24.0‰). However, the entrapped air volume of 3.3% (table 1) is appreciably lower due to the denser nature of the ice accreted on top of the hatch at this site.

### *Sample* F9

This sample was 1.9 cm thick and was obtained from the DTMB starboard forward bulkhead vertical panel. Compared with other samples collected during this icing event, the F9 sample was both the least dense (0.693 $Mg\,m^{-3}$) and the least saline (11.5‰). Combined with an estimated *in situ* measurement temperature of −8 °C, the density–salinity characteristics of the ice yielded a derived value of 25.7% for the entrapped air volume, but only 5.7% for the volume of brine trapped in the ice. The mean size of bubbles in the ice (0.29 mm) was also the largest measured in any sample from the February icing event. The crystal size was also the largest measured, as indicated in table 2. An additional feature of the microstructure of this sample of accreted ice is the widespread occurrence of polygonal crystals. These occur *in lieu* of less regular, or even shapeless, grains that could be expected of water droplets when they impact and freeze on the deck or superstructure of a ship. Most of the grain boundaries show minimal curvature, and 120° multigrain interactions are dominant. It cannot be determined just when this apparent conversion from rounded to polygonal grains occurred, but the fact that it has occurred emphasizes the importance of thin sectioning samples as soon as possible after the initial accretion has occurred, or even during the accretion process, in order to capture the true condition of the crystal structure. As also applies to previously discussed samples (F1, F3, F4 and F6), no preferred orientation of crystals was apparent, based on observations of the pattern of interference colours displayed when crystals are rotated between crossed polarizers.

### *Sample* M3

This sample was retrieved from the vertical front face of the 5″ gun and below the barrel. The thickness of the accreted ice was 1.1 cm when sampled. A bulk density of 0.848 $Mg\,m^{-3}$ was measured, which, in conjunction with a measured bulk salinity of 14.8‰ and an *in situ* ice temperature of −2.2 °C, gave derived values of brine and entrapped gas volumes of 30.1% and 11.3%, respectively. Microcrystalline characteristics indicate that this sample also suffered modification of its original grain structure since it was accreted. These modifications include substantial straightening of grain boundaries and formation of 120° triple junctions. These changes have not been accompanied by any significant preferred orientation of the component crystals. Crystal cross-sections and derived diameters averaged 0.58 $mm^2$ and

0.76 mm, respectively. Bubble diameters averaged 0.27 mm. Large numbers of irregularly shaped grains, including some that encircle crystals, are identified as brine inclusions.

### *Sample* M5

This sample was retrieved from the 5″ gun, as was sample M3, but was located at a more elevated level: 91 cm above the deck on the port side of the gun housing. This difference in location is clearly evident in both the ice thickness, only 0.6 cm, and the microstructural characteristics of sample M5. This ice exhibits a granular texture of well-rounded grains exhibiting the smallest crystal size of any sample of accreted ice collected on the cruise. The mean crystal cross-section measured 0.31 $mm^2$, which converts to an RMS diameter of 0.56 mm. In this particular section, the grains appear substantially immersed in brine, forming channel-like networks similar to the situation observed in samples M6 and M12 in figure 3. The ice also contained many rounded, presumed bubbles of air with a mean diameter of 0.27 mm. A mean density of 0.871 $Mg\,m^{-3}$ was measured in conjunction with a bulk salinity of 10.3‰.

### *Sample* M10

This sample (figure 7), measuring 3.4 cm thick, was taken from a bulkhead located on the port side of the 5″ gun at a height of 0.9 m above the deck. Thick sections cut perpendicular to the accretion surface show evidence of layering. A relatively low bulk salinity of 7.0‰ was measured; this, in conjunction with a measured density of 0.882 $Mg\,m^{-3}$ at $-3\,^{\circ}C$ (*in situ*), yields derived values of 10.8% and 5.3% of brine and entrapped air volume, respectively. The microstructure is composed of a mixture of rounded grains and straight-sided crystals exhibiting occasional 120° intersections. The latter would indicate partial recrystallization of the ice at some stage of its structure evolution. A mean cross-sectional area of crystals of 0.58 $mm^2$ (and its diameter equivalent of 0.76 mm) was measured in conjunction with a mean bubble diameter of 0.24 mm.

### *Sample* M11

This example of an icicle formed on a polypropylene lifeline was collected at a location forward of the 5″ gun mount immediately port of the windlass. The sample was *ca.* 6 cm long and 8 cm wide, and was hanging down and away from the relative wind (winds were from the port bow) (figures 8 and 9). Brine was dripping from the icicle, and it was very firm and difficult to remove from the polypropylene lifeline. A vertical section, cut longitudinally through the length of the icicle, is shown here photographed between crossed-polarizers (figure 8). Microstructure is characterized by grains elongated longitudinally down the length of the icicle, occasionally consisting of several crystals measuring several millimetres in length (see also figure 9). An intermixing of these elongated grains with smaller rounded grains is also featured in this section. A bulk salinity of 11.8‰ was measured. The thin section gives the impression of grains substantially immersed in brine.

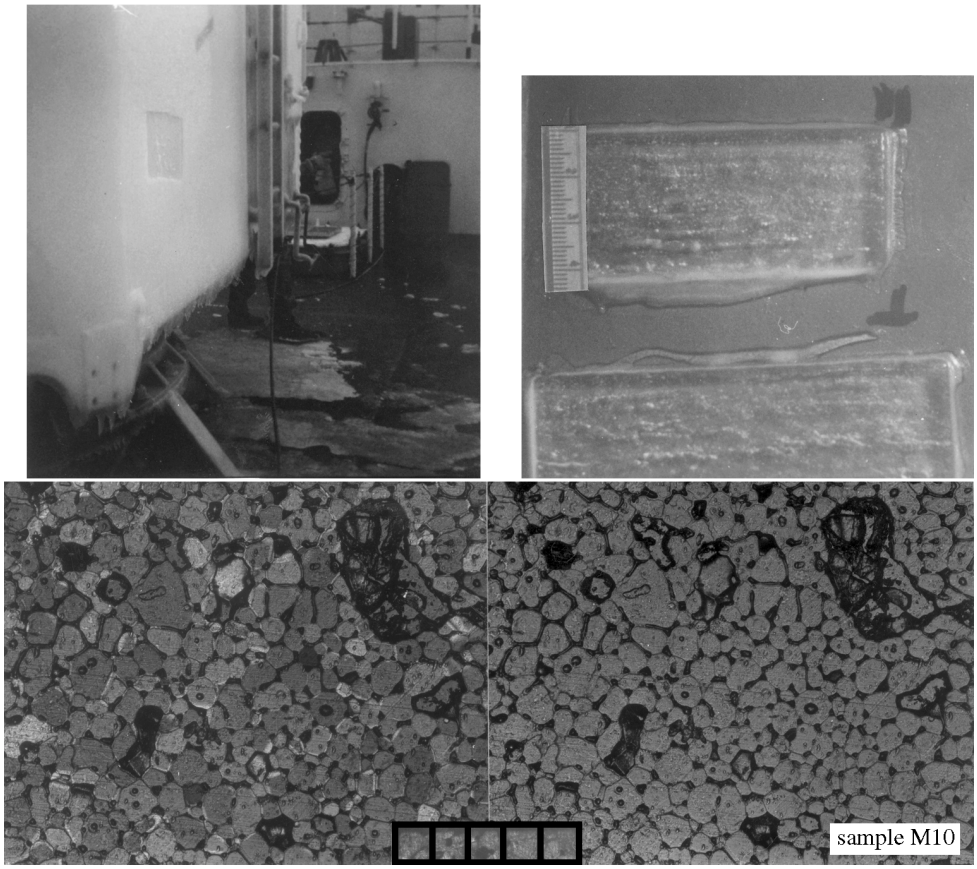


Figure 7. Sample M10 taken from the port bulkhead of the 5″ gun *ca.* 1 m above the deck (upper-left photograph). Thick sections suggest layering, and thin sections show a mixture of rounded and recrystallized ice crystals. The dark structure in the upper-right corner of the section is due to the coalescing of several brine pockets (scale in mm).

### *Sample* M12

This sample was retrieved from one of many icicles dripping from the bottom of the 5″ gun mount. The icicle sample appears to be two or more merged icicles. Brine was dripping from the icicles as they were removed. Crystals appear to radiate from two dark nodes, assumed to be drip tubes for the two icicles, and swirl counterclockwise around the left drip tube. Swirling does not appear around the right tube. Crystals appear to radiate outward from each drip tube outside of the swirl zone. A particular feature of the microstructure of this icicle is the incorporation of large millimetre-sized grains among much smaller grains. These two contrasting types of crystal were analysed separately for grain size; results are presented in table 2. A bulk salinity of 14.2‰ was measured on one of the icicles.

### *Sample* M13

This sample of deck icing (figure 10) was obtained from ice that had accreted to a thickness of 2.4 cm, *ca.* 2 m in front of the 5″ gun. Microstructurally, it consists of

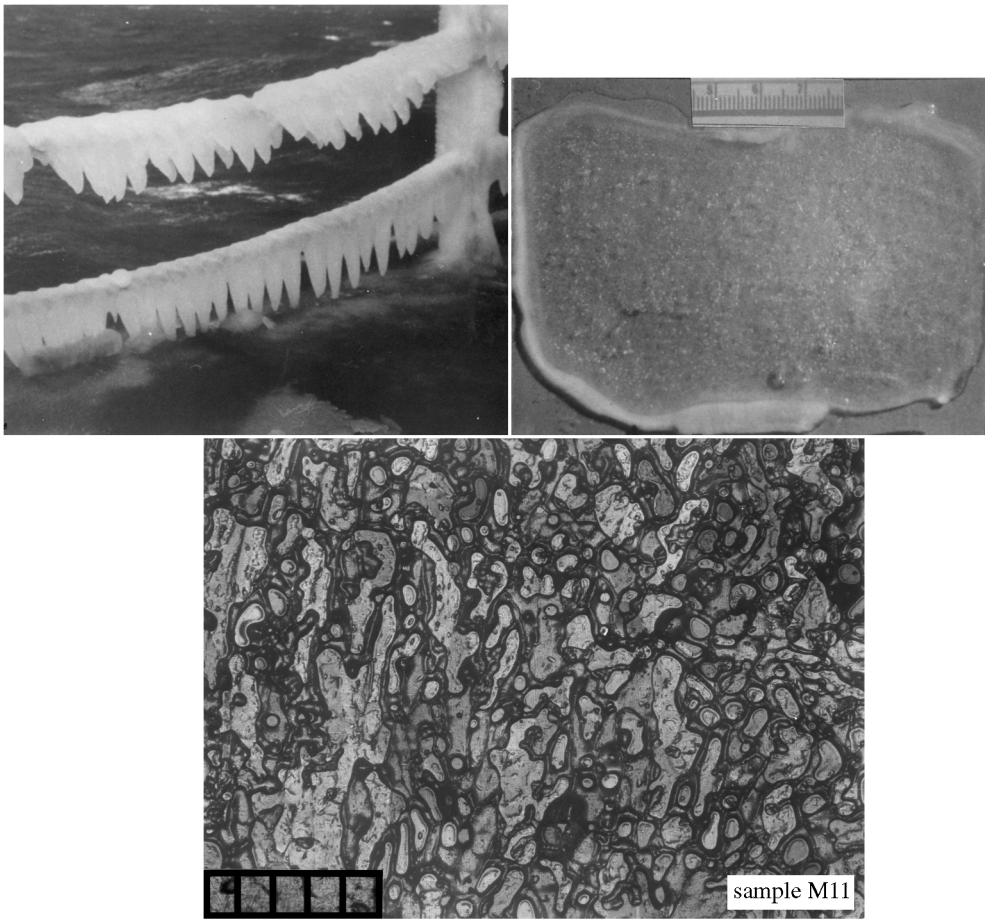


Figure 8. Sample M11 is taken from an icicle removed from the left end of the upper lifeline in the upper-left photograph. The upper-right photograph shows a horizontal section through the icicle in natural light, and the lower photograph shows a vertical cross-section with a mixture of rounded and elongated crystals as observed between crossed polarizers (scale in mm).

an intermixture of large, somewhat shapeless crystals with much smaller subrounded grains. The coarser crystals were among the largest measured in any sample collected on the cruise. They were certainly the largest observed in deck-accreted ice (table 2). In coarsely crystalline deck samples, such as those illustrated by this sample, layering is present but sometimes lacks continuity. A bulk salinity of 13.7‰ was measured, which, when used in conjunction with a density of 0.865 $\mathrm{Mg\,m^{-3}}$ and an *in situ* temperature of −1.6 °C, gives values of 40.1% and 10.3% for the volumes of brine and air incorporated into the ice, respectively. A mean gas bubble diameter of 0.25 mm was also measured.

### *Sample* M14

Several samples of ice were retrieved from this particular location situated 122–152 cm above the deck on the front face of the 5″ gun immediately under the barrel. The sample analysed here measured 1.1 cm in thickness. Excluding the icicles, this

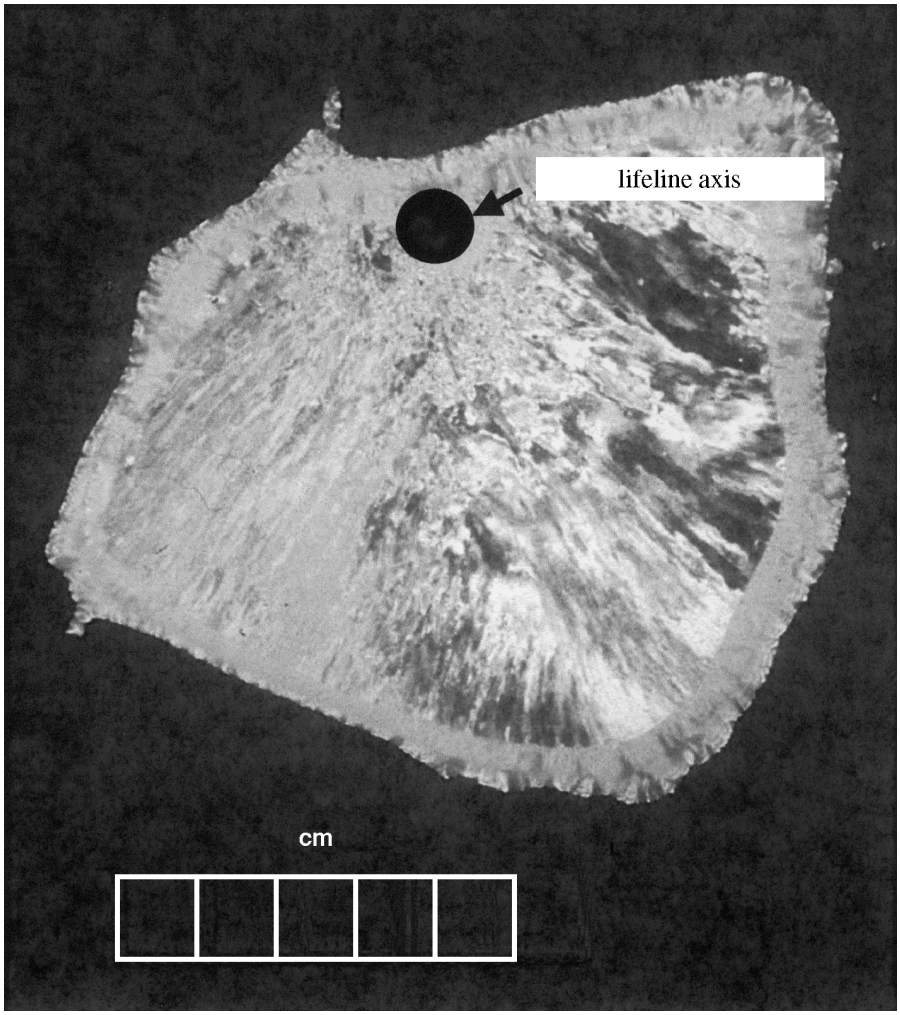


Figure 9. Vertical section of icicle, sample M11, photographed between crossed polarizers. Note the small round ice crystals near the lifeline, and the elongated crystals radiating away from the lifeline. The outermost layer around the sample is an artefact of mounting the sample on a glass slide (scale in cm).

sample contained the largest crystals of all the accreted ice that we examined; they averaged 1.05 $mm^2$ in cross-section, which converts to an RMS diameter of 1.02 mm. Microstructurally, the ice in this particular sample appears to have undergone some incipient recrystallization. A density of 0.827 Mg $m^{-3}$ was measured, which, together with a bulk salinity of 9.8‰ measured at the *in situ* temperature of the sample, yields derived values for the brine and entrapped air volumes of 15.2% and 12.0%, respectively. A mean gas bubble diameter of 0.24 mm was also measured, which is about four times smaller than the average size of crystals.

A selection of colour thin-section photographs of shipboard accreted ice, in addition to those featured in black and white format in figures 4–10, are presented in figure 11. Textures (variations in sizes and shapes of grain) range from well rounded

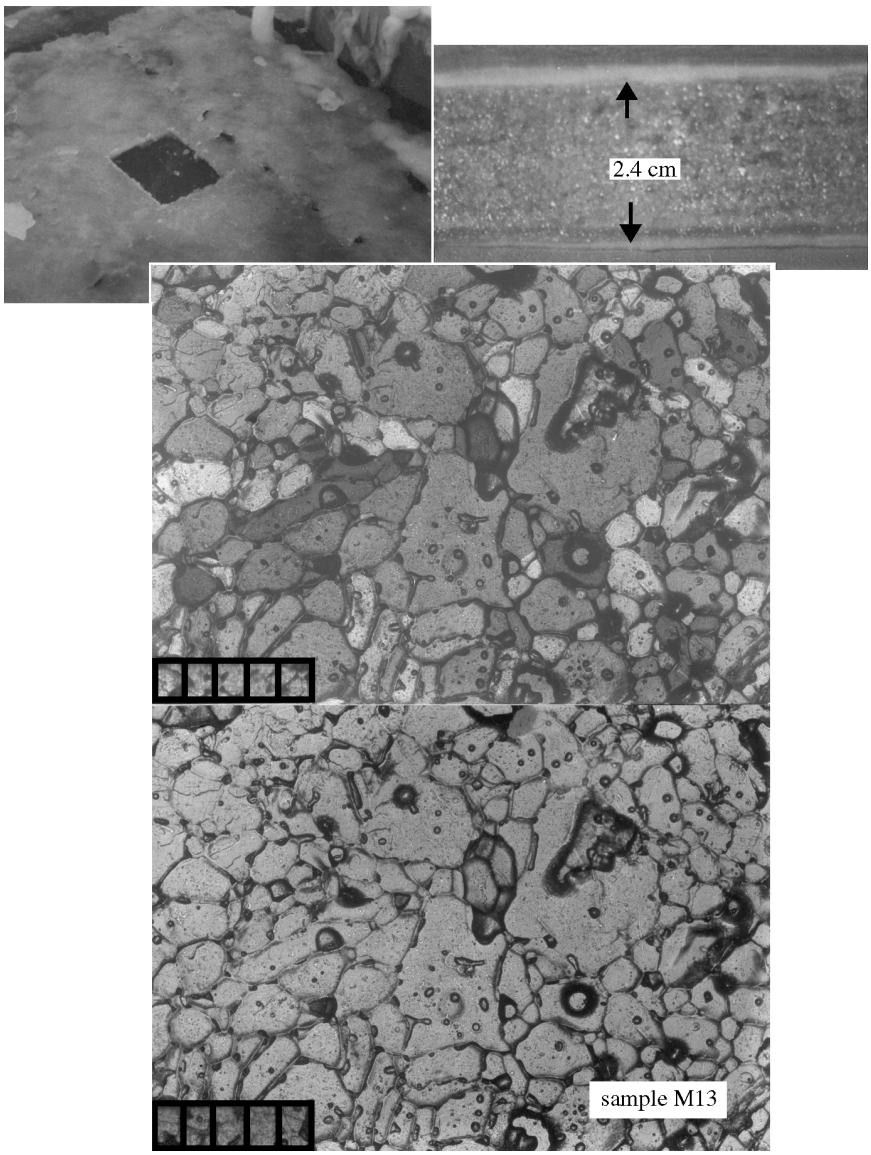


Figure 10. Sample M13 was removed from the deck in warm air temperatures, near −3 °C. Note the mixture of small crystals, and large irregular crystals. Approximately 50% of the sample consisted of pores filled with brine or air (scale in mm).

to polygonal. Mixtures of these two textures are also observed. An enlargement of the radial crystal structure characterizing the icicle cross-section in figure 10 is also shown.

## 12. Discussion and conclusions

Ice accreted on horizontal and vertical surfaces of USCGC *Midgett* ranged from densely packed (0.9 Mg m$^{-3}$) to loosely consolidated (0.7 Mg m$^{-3}$). Texturally, ac-

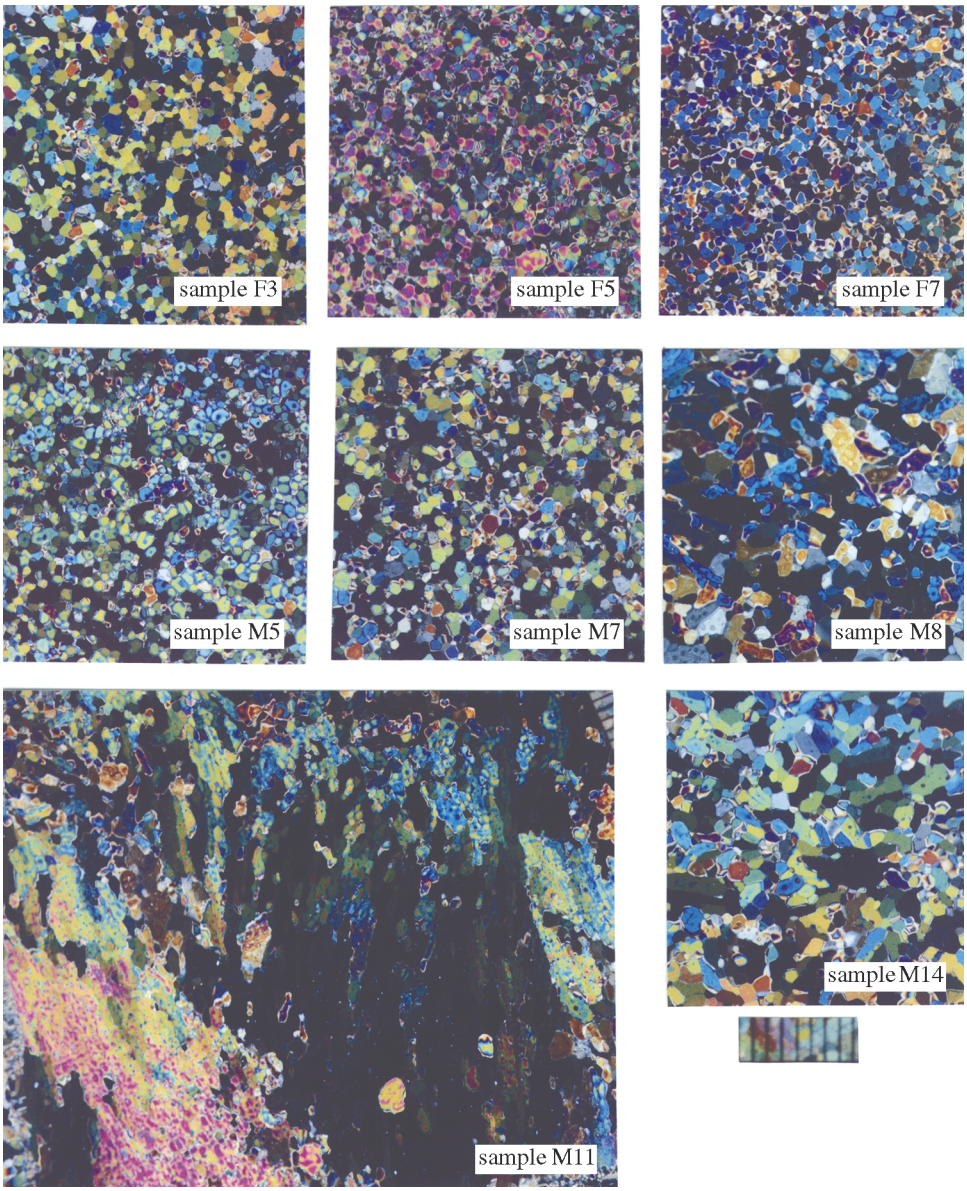


Figure 11. Thin-section photographs of representative samples of ice accreted to the deck and bulkhead surfaces of the USCGC *Midgett*. For characteristics of each sample, see tables 1 and 2. The scale beneath sample M14 is in millimetres, and applies to all thin-section photographs in this figure except M11, which is photographed at a 20% smaller scale.

creted ice clearly resembled frazil ice, formed from the consolidation of freely nucleated ice crystals in sea water. This resemblance is also reflected in the ratios and magnitudes of incorporation of brine. Bulk salinities ranged from 25.4 to 7‰, compared with values of 6–7‰ measured in normal sea ice. However, in frazil ice formed on the surface of the ocean, which frequently represents the initial mode of freezing of sea water, bulk salinities can exceed 10‰. Shapes of grains composing the crys-

talline structure of accreted ice ranged from rounded to polygonal. The observation that ice formed during the initial stages of accretion frequently displayed a polygonal crystalline structure can probably be attributed to thermally driven modification of the original microstructure, due, possibly, to heat leaking from the interior of the vessel. This process is generally manifested in terms of crystal boundary straightening, and the formation of triple junctions intersecting at equilibrium angles of *ca.* 120°, as observed in thin sections.

No trend towards a preferred orientation of crystallographic *c*-axes, either in freshly accreted ice or its thermally modified (recrystallized) variant, was observed. Mean grain dimensions ranged from a minimum value of 0.56 mm to 1.15 mm. The only exception was icicle-type ice, where the dimensions of crystals often exceeded several millimetres and where dimensional orientation (elongation of crystals in a preferred direction) was a commonly observed feature of the microstructure. Excluding the icicles, the mean dimensions of crystals accreted on both horizontal and vertical surfaces of the USCGC *Midgett* were similar to those measured by Tabata *et al.* (1963) but generally much larger than those derived from three-dimensional measurements of crystals reported by Golubev (1972). Golubev also reported significant levels of preferred orientation of the crystallographic *c*-axes. We did not, nor does this appear to be the case of observations of *c*-axis orientation in accreted ice examined by Tabata *et al.* (1963).

Estimates of brine volume and entrapped air content derived from measurements of the salinity, density and *in situ* temperature of samples, in conjunction with the equations of Cox & Weeks (1983), indicated wide-ranging values, as expected in view of the wide-ranging values of density, salinity and temperature.

All measurements of superstructure bow spray icing prior to the *Midgett* research cruise were made on fishing trawlers or small patrol boats, vessels with displacements 25% or less of the cutter's 2703 t. However, few measurements have been made of superstructure saline ice structure and properties on any size of ship. Those prior studies, only two in number, were made by the Soviets and Japanese 20 and 30 years ago, respectively. The most detailed of the two studies was by the Soviets, the Japanese only discussing ice structure briefly.

Though icing rates experienced on the *Midgett* were low, and ice thicknesses were small, useful measurements were made. Ice thickness was greater on decks than on bulkheads, with an approximate ratio of 1.25:1 between deck and bulkhead ice thickness. If average ice density is also accounted for, the ratio of mass per unit area increases the ratio to 1.4:1, because the density of ice on decks was larger than on bulkheads. This ratio has serious implications for modelling superstructure icing, because higher levels on ships, where centre of gravity is most affected by ice, are dominated by bulkheads. Ice on horizontal surfaces (deck and hatch covers) of the *Midgett* also produced fewer and smaller inclusions than did ice on vertical surfaces (bulkheads).

Structure analysis of ice accreted around a polypropylene lifeline showed the largest ice crystals observed aboard the *Midgett*. Small, rounded, randomly oriented crystals dominated the ice mass immediately around the wire. Thereafter, long crystals grew radially to the outer edge of the elongated ice mass. The accretion visually resembled an icicle externally (Laudise & Barns 1979). The structure does appear similar to the crystal structure in freshwater glaze ice around hay stalks, where crystal growth is perpendicular to and radially oriented around the stalk (Ackley & Itagaki 1974).

In the case of glaze, heat loss is initially to the accretion surface, but eventually heat flow occurs into the atmosphere as ice thickness increases. Crystal growth is, thus, promoted in the direction of cooling, down the temperature gradient and towards the atmosphere.

Saline icicles actively grew below the 5″ gun housing. Externally, the icicles exhibit several features of freshwater icicles, including horizontal surface ribbing and pendant drops (Geer 1981). Internally, the icicles have features of freshwater icicles, and saline subaqueous stalactites (Weeks & Ackley 1982; Perovich *et al*. 1995). Crystal growth is radial away from and orthogonal to the long axis of the icicle, similar to some freshwater icicles (Laudise & Barns 1979). However, it is also similar in some respects to stalactites that form under sources of cold, highly saline brine, such as thick young ice (Perovich *et al*. 1995). In the latter case, cold brine flows through the stalactites within tortuous channels up to several cm in diameter. The channel is commonly frazil lined, with columnar crystals growing radially into the surrounding warmer water. The *Midgett* icicle brine tubes are surrounded by ice transitioning from frazil to elongated crystals that are approaching columnar in appearance and also growing radially. Processes that produce saline icicles have been modelled (Makkonen 1988; Lozowski *et al*., this issue), but detailed comparisons have not been made between stalactite and saline-icicle processes.

Ice properties on the *Midgett* were generally similar to those observed by the Soviets on trawlers. Salinity was higher on horizontal surfaces than on vertical surfaces. Ice density fell within the range of observations by the Soviets, and was somewhat lower on vertical surfaces than on horizontal surfaces. Following the ice salinity pattern, the percentage of ice pores filled with brine was greater on horizontal than on vertical surfaces, as calculated by the Cox & Weeks (1983) equations.

This project was supported by the US Navy Office of Naval Technology, and by the US Army Corps of Engineers under work item ‘Structure and Properties of Saline Spray Ice’. The crew of the USCGC *Midgett* and Lieutenant Commander P. Longo (retired, US Navy) provided valuable assistance during and after the cruise.

## References

Ackley, S. & Itagaki, K. 1974 Crystal structure of a natural freezing rain accretion. *Weather* **29**, 189–192.

Ahlmann, H. & Droessler, F. 1949 Glacier ice crystal measurements Kebnekajse, Sweden. *J. Glaciol.* **1**, 268–274.

Brown, R. & Roebber, P. 1985 The ice accretion problem in Canadian waters related to offshore energy and transportation. AES report no. 85-13, Downsview, ON, Canada.

Cox, G. & Weeks, W. 1983 Equations for determining the gas and brine volumes in sea-ice samples. *J. Glaciol.* **29**, 306–316.

Frankenstein, G. & Garner, R. 1967 Equations for determining the brine volume of sea ice from −0.5 °C to −22.9 °C. *J. Glaciol.* **6**, 943–944.

Gates, E., Narten, R., Lozowski, E. & Makkonen, L. 1986 Marine icing and spongy ice. In *Proc. IAHR Symp. on Ice, Iowa City, IA*, vol. 2, pp. 153–163.

Geer, I. 1981 The not-so-ordinary icicle. *Weatherwise* **34**, 257–259.

Golubev, V. 1972 On the structure of ice formed during icing of ships (from the materials of expeditions research). In *Issledovaniye Fizicheskov Prirody Obledeneniya Sudov, Leningrad*. CRREL Draft Translation TL411, 1974, pp. 108–116.

Gow, A. 1987 Restraints on thin section analysis of grain growth in unstrained polycrystalline ice. *J. Physique* **48**, 277–281.

Iwata, S. 1973 Ice accumulation on ships. In *Contributions, Arctic Oil and Gas: Problems and Possibilities*. In *5th Int. Congr. of the Fondation Française D'Etudes Nordiques, Le Havre, France, 2–5 May 1973* (ed. J. Malaurie), vol. 12, pp. 363–386.

Jorgensen, T. 1982 Influence of ice accretion on activity in the northern part of the Norwegian continental shelf. Offshore Technology Testing and Research report no. F82016. Trondheim, Norway: Continental Shelf Institute, Norwegian Hydrodynamic Laboratories.

Kultashev, Ye., Malakhov, N., Panov, V. & Shmidt, M. 1972 Spray icing of MFT and MFTF fishing vessels. In *Issledovaniye Fizicheskov Prirody Obledeneniya Sudov, Leningrad*. CRREL Draft Translation TL411, 1974, pp. 127–139.

Laudise, R. & Barns, R. 1979 Are icicles single crystals? *J. Crystal Growth* **46**, 379–386.

Makkonen, L. 1987 Salinity and growth rate of ice formed by sea spray. *Cold Regions Sci. Technol.* **14**, 163–171.

Makkonen, L. 1988 A model of icicle growth. *J. Glaciol.* **34**, 64–70.

Mellor, M. 1983 Mechanical behavior of sea ice. CRREL report 83-1.

Ono, N. 1968 Studies of ice accumulation on ships. Part 2. Conditions of icing and ice accretion weights. *Low Temp. Sci. (Teion Kagaku)* A **22**, 170–181. (Translated by E. Hope, National Research Council, Ottawa, Canada, Technical Translation 1319.)

Panov, V. 1972 On calculation of water droplet temperature and ice salinity during spray icing of ships. In *Investigation of the Physical Nature of Ship Icing*, *Issledovaniye Fizicheskov Prirody Obledeneniya Sudov, Leningrad*. CRREL Draft Translation TL411, pp. 42–48.

Perovich, D., Richter-Menge, J. & Morison, J. 1995 Formation and morphology of ice stalactites observed under deforming lead ice. *J. Glaciol.* **41**, 305–312.

Ryerson, C. 1991 Ship superstructure icing climatology of coastal eastern North America. In *Proc. 48th Ann. Eastern Snow Conf., Guelph, ON, Canada*, pp. 201–211.

Ryerson, C. 1995 Superstructure spray and ice accretion on a large US Coast Guard Cutter. *Atmos. Res.* **36**, 321–337.

Ryerson, C. & Longo, P. 1992 Ship superstructure icing; data collection and instrument performance on the USCGC Midgett research cruise. CRREL report 92-23.

Schytt, V. 1958 Glaciology. II. Inner structure of the ice shelf at Maudheim as shown by core drilling. *Norwegian–British–Swedish Antarctic Expedition, 1949–1952. Scientific results*, vol. IV C, pp. 113–148. Oslo: Norsk Polarinstitutt.

Seligman, G. 1949 The growth of the glacier crystal. *J. Glaciol.* **1**, 254–267.

Shellard, H. 1974 The meteorological aspects of ice accretion on ships. Marine Science Affairs, report no. 10 (WMO-no. 397). Geneva: World Meteorological Organization.

Smirnov, V. 1972 Conditions of ship icing and means of combating it (according to foreign data). In *Issledovaniye Fizicheskov Prirody Obledeneniya Sudov, Leningrad*. CRREL Draft Translation TL411.

Stephenson, P. 1967 Some considerations of snow metamorphism in the Antarctic ice sheet in light of ice crystal studies. In *Physics of Snow and Ice: Proc. Int. Conf. on Low Temperature Science 1966* (ed. H. Oura), vol. 1, part 2, pp. 725–740. Institute of Low Temperature Science, Hokkaido University.

Tabata, T., Iwata, S. & Ono, N. 1963 Studies of ice accumulation on ships. Part 1. *Low Temp. Sci. (Teion Kagaku)* A **21**, 173–221. (Translated by E. Hope, National Research Council, Ottawa, Canada, technical translation 1318.)

Weeks, W. & Ackley, S. 1982 The growth, structure, and properties of sea ice. USA Cold Regions Research and Engineering Laboratory, CRREL Monograph 82-1.